

# Molecular Weight Effects on Phase Behavior of Blends of Poly(phenylene oxide) with Styrenic Triblock Copolymers

P. S. Tucker, J. W. Barlow, and D. R. Paul\*

Department of Chemical Engineering and Center for Polymer Research, University of Texas at Austin, Austin, Texas 78712. Received December 28, 1987;  
Revised Manuscript Received March 10, 1988

**ABSTRACT:** The degree of solubilization of poly(2,6-dimethyl-1,4-phenylene oxide) (PPO) homopolymer in the polystyrene (PS) microphases of triblock copolymers has been investigated by differential scanning calorimetry while independently varying the PS block molecular weight (from 5300 to 87 000) and the PPO molecular weight ( $M_w$  from 23 900 and 39 000). The exothermic heat of mixing for PPO and PS units causes a dramatic increase in the extent of homopolymer solubilization relative to that found previously when the homopolymer was polystyrene. While the molecular weight of the PS block is a major factor determining the extent to which PPO and PS segments mix, the molecular weight of the PPO has little or no effect over the range investigated. This is also in contrast to what has been observed for the case of blending polystyrene into such block copolymers, and as shown in a companion paper, this is a direct consequence of the additional driving force for solubilization provided by the exothermic mixing of PPO and PS. Rubber block type, size, or location does not appear to have any major effect on solubilization within the limited range examined. Brief annealing resulted in only minor changes in phase behavior, indicating that these blends are not far removed from their equilibrium mixing state.

## Introduction

Over the past 2 decades, there have been numerous reports on blends of block or graft copolymers with homopolymers having repeat units identical with those of one or more of the segments of the copolymers.<sup>1-4</sup> A principal issue has been the extent to which homopolymers can be solubilized into the respective copolymer microphases as this relates to approaches for modification of the copolymer or the homopolymer and for emulsification or "compatibilization" of immiscible blends. Several experimental investigations have shown that the degree of solubilization is a strong function of the molecular weight of the homopolymer,  $M_H$ , relative to that of the corresponding copolymer segment,  $M_A$ , with significant solubilization being possible only when  $M_H/M_A$  is unity or less. Since mixing of say homopolystyrene with a polystyrene block of a copolymer is an athermal process, the thermodynamic factors favoring and opposing solubilization in this case are various entropic ones in addition to the unfavorable enthalpy of mixing for the same unlike segments that drives phase separation of the copolymer itself. Statistical thermodynamic theories<sup>5-9</sup> which approximate the various factors lead to results in at least semiquantitative accord with these experimental observations.

Only a relatively few studies<sup>10-15</sup> have dealt with the case where the homopolymer, H, is different chemically from all of the copolymer segments but can form miscible blends with the A block material, e.g., H = poly(2,6-dimethyl-1,4-phenylene oxide) (PPO) and A = polystyrene (PS). Homopolymers of PPO and PS are well-known to form miscible blends for all proportions, molecular weights, and temperatures.<sup>16-18</sup> This case differs from the well-studied one of A = H in at least two important ways. First, miscible but unlike H and A structures are likely to involve an exothermic enthalpy of mixing<sup>19</sup> that can be an important additional thermodynamic driving force for solubilization. Second, the glass transition temperatures for H and A can be appreciably different as they are for PPO and PS. This permits measurement of  $T_g$  as a tool for investigating phase behavior of copolymer-homopolymer blends. More importantly this offers opportunities for meaningful improvements in the thermal properties of the A domains. For example, the upper use temperature of thermoplastic elastomers with polystyrene end blocks is

Table I  
PPO Characteristics

designation used here	$M_n^a$	$M_w^a$	$M_z^a$	$[\eta]^b$ dL/g	$M_w/M_n$	$T_g^c$
PPO-24	15 500	23 900	33 400	0.379	1.54	219.8
PPO-31	15 000	31 200	58 900	0.461	2.08	219.0
PPO-33	17 900	32 900	53 900	0.476	1.83	220.5
PPO-34	22 600	34 000	57 200	0.499	1.50	219.6
PPO-39	29 400	39 000	59 900	0.525	1.33	223.2

<sup>a</sup> Results by laser light scattering GPC. <sup>b</sup> In chloroform at 25 °C.  
<sup>c</sup> Transition midpoint by DSC at 40 °C/min.

limited by the  $T_g$  of the PS domains. Addition of PPO to this phase can raise its softening point<sup>10</sup> and extend the upper end of the useful temperature range for such thermoplastic elastomers.<sup>20</sup>

Earlier studies have shown that PPO seems to form a completely mixed phase with the polystyrene end blocks of thermoplastic elastomers for all blend proportions in some cases<sup>11</sup> but not in others.<sup>14,15</sup> The distinction in these cases seems to be related to the relationship of  $M_H$  versus  $M_A$ . However, we expect this relationship to be altered from that described above for A = H = PS because of the additional enthalpic driving force for mixing when H = PPO and A = PS. The purpose here is to map the extent of mixing of PPO with polystyrene blocks of copolymers of various architectures as a function of both  $M_H$  and  $M_A$ . This is done by examining the glass transition behavior of the hard phase by using differential scanning calorimetry.<sup>21</sup> A companion paper formulates a simple model that approximates the various thermodynamic factors believed to influence the extent of mixing of the hard-phase components. The experimental results given here are in good semiquantitative accord with the main predictions of the model.

## Experimental Section

The poly(phenylene oxide) (PPO) materials used in this investigation, see Table I, were kindly donated by Dr. Joseph C. Golba, Jr., of the General Electric Co. Molecular weight characteristics were determined by laser light scattering gel permeation chromatography for us by Dr. Joseph C. Golba and Dr. Peter C. Juliano. Solution intrinsic viscosities were determined at 25 °C in chloroform by using an Ostwald-Fenske viscometer. The glass transition temperatures shown were obtained by differential scanning calorimetry, DSC, at 40 °C/min as described below. The

Table II  
Triblock Copolymer Characteristics

designation used here	commercial designation	end-block MW	midblock MW	% PS
SEBS-5	exptl	5 300	69 000	13.3
SEBS-7	exptl	7 200	34 000	29.8
SEBS-8	Kraton G1652	7 500	37 500	28.6
SEBS-10	exptl	10 000	47 000	29.9
SBS-15	Kraton D1101	14 500	67 500	28.8
SEBS-29E	exptl	29 000	118 000	33.0
SEBS-29C	Kraton G1651	29 000	116 000	33.3
ISI-87	exptl	47 000	87 000	48.0

PPO samples were chosen for their range of molecular weights with the highest being nearly twice that of the lowest. The PPO designations indicate the nominal weight-average molecular weight in thousands, e.g., PPO-33 indicates the sample with  $M_w = 32900$ .

Blends spanning the entire composition range were prepared from each of the PPO samples with each of eight triblock copolymers, listed in Table II, donated by G. Holden and Vivek Soni of the Shell Development Co. Molecular weight characterization was provided with the experimental materials and is available from several sources in the literature<sup>11,14,22-24</sup> for the commercial materials. Most of the copolymers have polystyrene (PS) end blocks and a hydrogenated polybutadiene midblock that is essentially a random copolymer of ethylene and butylene, hence the designation SEBS. The SBS copolymer shown as polystyrene end blocks and a polybutadiene midblock (not hydrogenated) while the ISI copolymer has hydrogenated polyisoprene end blocks and a polystyrene midblock. The number following the letter designation is the nominal PS molecular weight in thousands. Distinction is made between the two copolymers having identical PS molecular weight by a "C" denoting commercial and an "E" denoting experimental materials.

The components, in the desired proportions, were dissolved in a 3:1 mixture by weight of toluene and chloroform to produce a 5% polymer solution and then precipitated at 40 °C into an excess of methanol. At this temperature, all solutions were completely clear. The precipitates were filtered, air dried for 24 h, and vacuum dried for 48 h at 60–70 °C. Approximately seven compositions for each of 36 blend systems were prepared and tested. ISI-87 was blended with only PPO-33 due to the limited quantity of this block copolymer.

Phase behavior of each system was investigated by differential scanning calorimetry. Dried precipitates weighing 10–20 mg were encapsulated in aluminum pans for measurement using a Perkin-Elmer DSC 2 equipped with a thermal analysis data station for the systems SEBS-8/PPO-34, SBS-15/PPO-34, and SEBS-29C/PPO-34, while a Perkin-Elmer DSC 7 was used for all other systems. The temperature region encompassing the glass transitions of the PS block and the PPO homopolymer was investigated. Scans utilizing base-line subtraction for improved clarity were obtained on heating at 40 °C/min subsequent to cooling from a high temperature at the same rate. This scan rate was chosen to increase the sensitivity of the output as described in a previous paper.<sup>14</sup> Transition temperatures remained constant for the same samples during repeated scans in this manner, leading to the conclusion that solvent removal was essentially complete. Compositions examined by using the DSC-7 were subsequently cooled to a temperature 10 °C below the  $T_g$  predicted by the Fox equation for a completely mixed hard phase, annealed for 30 min, cooled at 40 °C/min, and then thermally scanned again. The glass transition temperature was taken as the mean of the onset and end-point temperatures, defined by the intersections of extrapolated base lines below and above the transition with the tangent through the inflection of the transition. The breadth of the transition,  $\Delta T_g$ , is equal to the difference in end-point and onset temperatures. The change in heat capacity through the transition,  $\Delta C_p$ , is the vertical height between extrapolated base lines at the  $T_g$ .

## Results and Discussion

The approach used here is to examine samples by DSC for  $T_g$  behavior within the region between the transitions for the two hard-phase components, PS and PPO. The

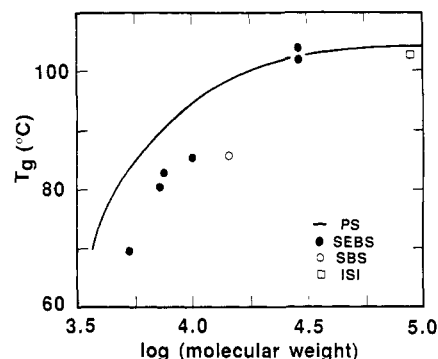
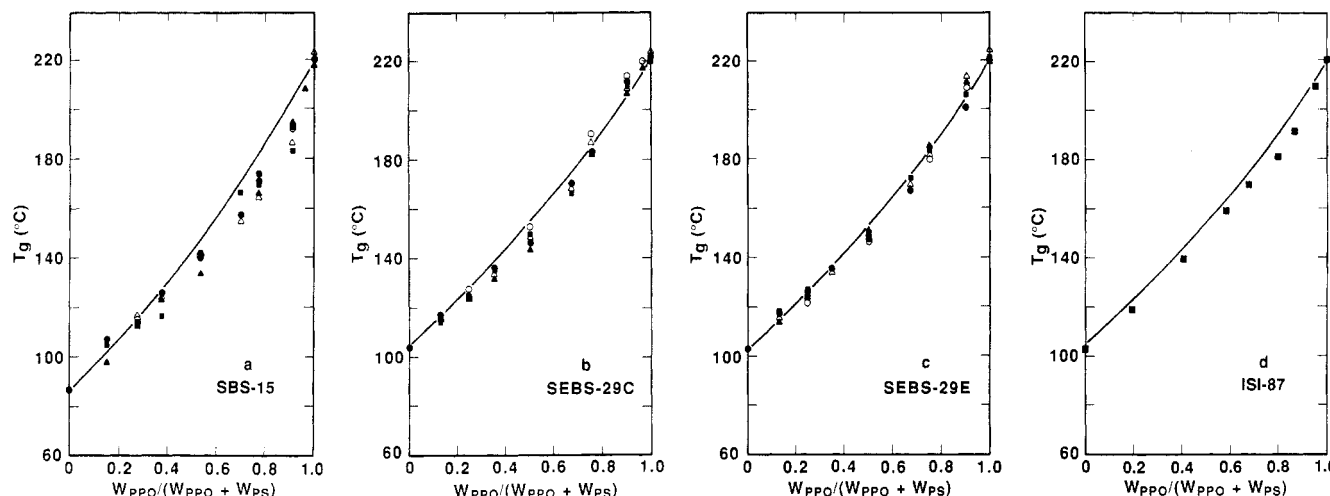


Figure 1. Glass transition temperatures by DSC at 40 °C/min for the styrenic phase of triblock copolymers as a function of PS block molecular weight. Polystyrene homopolymer behavior for the same conditions is represented by a solid line.

glass transitions observed for the PS phase of the pure block copolymers are described first. Next, results are given for blend systems that exhibited a single hard-phase glass transition which is indicative of essentially complete mixing of the PPO with the PS phase of the copolymer. Finally, a series of blends are described that exhibited two glass transitions at high PPO contents caused by two separate hard phases. The breadth and heat capacity changes of the glass transitions are shown to gain additional insight about the hard phases of the blends. In the following discussions, the overall PPO content of the blends is expressed as a fraction of the hard-phase components, i.e., on a rubber-free basis, to facilitate comparisons with PPO-PS homopolymer blends.

**Pure Copolymers.** Figure 1 shows the hard-phase glass transition temperature of the copolymers in Table I as a function of the PS block molecular weight. Solid circles represent SEBS copolymers while the open circle and open square are values for SBS and ISI, respectively. The solid line represents homopolystyrene transition behavior for the same conditions.<sup>14</sup> The glass transition temperature of the PS block of a phase-separated copolymer depends upon molecular weight in a manner similar to that of PS homopolymer but is lower in magnitude initially than for homopolystyrene with the same molecular weight.<sup>24</sup> As the molecular weight becomes larger, the  $T_g$  of the PS block approaches the homopolymer value.<sup>24</sup> The depression of the  $T_g$  for PS microphases has been attributed to surface energy effects,<sup>25</sup> the diffuse interphase between the domain and matrix phase,<sup>24</sup> and the mixing of rubbery segments in the glassy domain.<sup>24,26</sup> While it has been demonstrated that the molecular weight of the rubbery phase and the architecture (diblock or triblock) have negligible effect on the PS transition,<sup>26</sup> the type of midblock appears to affect the transition temperature at low molecular weights since the  $T_g$  for SBS-15 is significantly lower than expected on the basis of the trend for the SEBS transitions. This observation is reasonable since the magnitude of the repulsion between segments will affect the surface energy, the diffuseness of the interphase, and the mixing of the rubbery component in the glassy phase. The solubility parameter difference between PS and hydrogenated PB is about twice that for PS and PB; thus, the SBS-15 copolymer has a weaker repulsion between segments than the SEBS materials causing an increase in the interphase volume, an increase in the mixing in of the rubbery component, and, ultimately, a lower transition for the hard phase, as observed in Figure 1.

**Systems with a Single Hard-Phase Glass Transition.** The glass transition behavior for blends of four block copolymers with the various PPOs is shown in Figure 2



**Figure 2.** Hard-phase glass transition temperatures by DSC at 40 °C/min versus weight fraction of PPO (on a rubber-free basis) for blends of PPO-24 (●), PPO-31 (▲), PPO-33 (■), PPO-34 (○), and PPO-39 (△) with block copolymers in order of increasing PS block molecular weight where (a) is SBS-15, (b) SEBS-29C, (c) SEBS-29E, and (d) ISI-87. Data points are averages of several determinations. All systems display a single hard phase at each composition. The solid line represents the Fox prediction for  $T_g$ .

as a function of the weight fraction PPO in the hard phase. The solid lines represent predictions by the Fox equation<sup>27</sup> calculated from the end points. This prediction satisfactorily describes the glass transition behavior for PPO/homopolystyrene blends<sup>16</sup> and is shown for comparison. A single, composition-dependent  $T_g$  is observed for each blend system in this figure, suggesting the presence of only one hard phase composed of PS block segments and PPO chains. These four copolymers have the highest PS block molecular weights of the eight copolymers in Table II; however, the glass transition behavior appears to be independent of the particular PPO used since no trend with PPO molecular weight is detectable.

The general shape of the data for the SBS-15 blends (Figure 2a) follows the Fox prediction for miscible blends, although at high concentrations of PPO the data lie slightly below this prediction as reported before.<sup>14,15</sup> The SBS-15/PPO-34 system (solid circles in Figure 2a) has been investigated by dynamic mechanical analysis and scanning transmission electron microscopy, STEM, in a previous paper.<sup>15</sup> STEM results indicate the presence of an essentially pure PPO phase at high contents of this component, but the amount of this phase was evidently too small to be detected by either DSC or dynamic mechanical analysis. Glass transition temperatures slightly below the expected  $T_g$ s were the only evidence by the latter methods that a second PPO-rich phase might exist. The other PPO materials blended with SBS-15 show a similar deviation from the Fox prediction at high PPO contents so the presence of a small amount of PPO-rich phase cannot be ruled out or confirmed on the basis of this single method of analysis.

Transition data for blends of PPO with SEBS-29C and with SEBS-29E (Figure 2b,c) are virtually identical, as might be expected since the block copolymer materials have the same PS block molecular weight and nearly identical midblock molecular weights. No trend with PPO molecular weight is obvious for either copolymer. The overall pattern of the data is sigmoidal, with the observed points lying below the predicted transition temperature at the middle compositions and above at higher PPO concentrations. Similar behavior has been observed for homopolymer blends<sup>28</sup> as well as for block copolymer/homopolymer systems.<sup>14</sup> In our case, the use of onset, midpoint, or end-point temperature to describe the transition leads to similar curves.

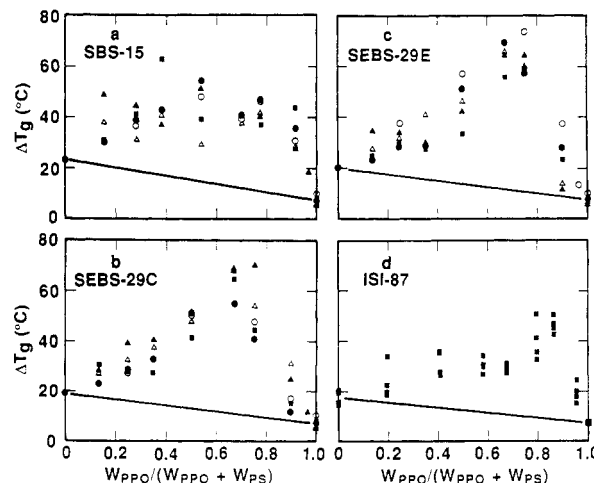


**Figure 3.** Breadth of the hard-phase glass transition versus weight fraction of PPO for blends of Figure 2, where (a) is SBS-15, (b) SEBS-29C, (c) SEBS-29E, and (d) ISI-87, with PPO-24 (●), PPO-31 (▲), PPO-33 (■), PPO-34 (○), and PPO-39 (△). Data points are averages of several determinations in (a), (b), and (c) but are individual determinations in (d). Tie line is shown for reference.

For ISI-87, blends were prepared only with PPO-33 for reasons already mentioned. This system, shown in Figure 2d, exhibits a single transition for each composition having an overall pattern similar to that for SBS-15 in Figure 2a. The ISI material was included in this study to determine whether the location of the PS block in the copolymer had any dramatic effect on ability to mix with PPO. A wider range of PS block molecular weights is needed to fully explore this notion.

From the results shown above, it appears that the polystyrene segments in these four block copolymers mix rather completely with any of the PPO samples in Table I to form a single hard phase. Based on the prior STEM work mentioned,<sup>15</sup> a very small amount of an additional PPO-rich phase is possible at high PPO contents although none was detected by DSC.

The breadths of the  $T_g$  regions for these blends are shown in Figure 3 as a function of PPO fraction. The points are averages of several determinations for each blend. Tie lines connecting the composition extremes are shown for reference. The breadth of the glass transition

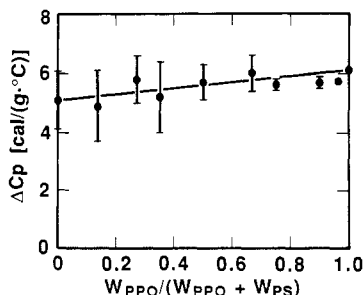


**Figure 4.** Average and standard deviation of heat capacity change through the  $T_g$  versus weight fraction of PPO for the blends of each homopolymer with SEBS-29C. The points are averages for multiple determinations and for different PPO samples while bars indicate the standard deviation about their averages.

region is normally greater for miscible blend than simple additivity of the pure component breadths. Short-range compositional fluctuations which exist even at equilibrium have been suggested to account for this behavior.<sup>29</sup>

Breadths for blends of SBS-15 with each PPO, shown in Figure 3a, increase smoothly to a maximum between 55 and 80 wt % PPO. Although there is scatter, no trend with PPO molecular weight is apparent. Figure 3b,c shows similar behavior for these two nearly identical copolymers. Generally, the data are concave upward from both composition extremes to a peak at around 70 wt % PPO where  $\Delta T_g$  is nearly 60 °C greater than expected by simple additivity. This sharp peak was not observed for the blends with the copolymer having a polybutadiene midblock, which may indicate some difference in the mixing behavior of PPO with the PS blocks. There are also some slight differences in the shapes of the  $T_g$  versus composition curves for blends based on the two SEBS copolymers relative to those based on SBS. Breadths for the ISI-87/PPO-33 system (Figure 3d) have characteristics of both the SBS and the SEBS blends. There is a smooth increase with downward concavity up to about 70% PPO, then the breadth increases to a peak around 85% PPO similar to the SEBS blends. Data points in this plot are individual determinations of  $\Delta T_g$  and not averages as in the other three plots. The scatter of these individual points is comparable to that of the averages for the different PPOs in Figure 3a–c. Thus, the scatter in all cases is related to experimental reproducibility and not PPO type. At all compositions, the deviation of  $\Delta T_g$  from additivity is generally smaller for blends with the ISI copolymer, which has the highest PS segment molecular weight, than with the other copolymers. All of these systems show much larger  $\Delta T_g$ s than can easily be accounted for by short-range compositional fluctuations. Longer range composition gradients that span the dimensions of the domains, as proposed by Jiang et al.<sup>9</sup> and supported elsewhere,<sup>15</sup> probably contribute to the observed transition broadening.

The changes in heat capacity,  $\Delta C_p$ , over the  $T_g$  region for the different pure PPOs vary only slightly and compare well with values reported by others.<sup>28</sup> The copolymers show considerable differences in the  $\Delta C_p$  at the  $T_g$  of their microphases. When normalized for the mass of PS present, these values are all lower than that reported for PS homopolymer<sup>28</sup> except in the case of the copolymer having the highest PS block molecular weight, ISI-87, whose value approaches that of the homopolymer. These values probably reflect differing contributions from segment mixing and from the interphase regions.

Figure 4 shows  $\Delta C_p$  (based on total hard-phase mass) results for blends of one of the block copolymers with PPO. The points are averages for several determinations on the same sample and for samples prepared from the different

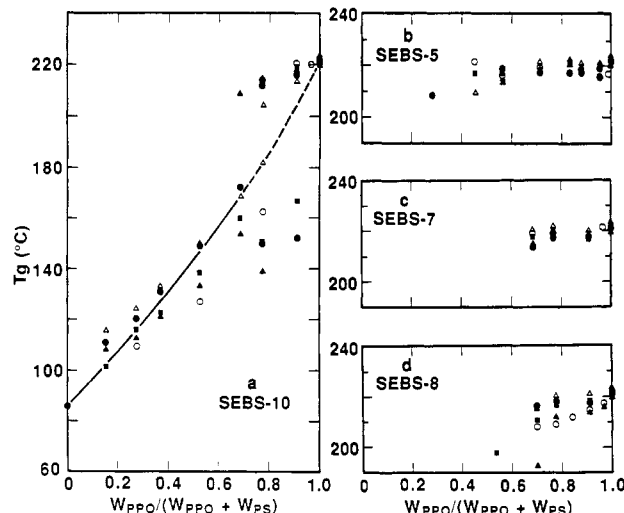


**Figure 5.** Hard phase glass transition temperatures by DSC at 40 °C/min versus weight fraction PPO for blends of PPO-24 (●), PPO-31 (▲), PPO-33 (■), PPO-34 (○), and PPO-39 (△) with block copolymers: (a) SEBS-10 (line shown is the Fox prediction), (b) SEBS-5; (c) SEBS-7; (d) SEBS-8. Both upper and lower hard-phase transition temperatures are shown in (a), while only the upper hard-phase transition is shown in (b), (c), and (d). All systems exhibit a region over which two hard phases are detected.

PPOs in Table I. The bars denote the standard deviations which were the same from PPO to PPO as from multiple determinations on the same sample. The standard deviations are higher the lower the PPO content. The trend of these data is very close to the additive line drawn. There is some possibility that the deviations below additivity at high PPO contents are statistically significant and could, therefore, reflect a minute amount of a pure PPO phase as observed previously by STEM.<sup>15</sup> The trends for blends with the other copolymers are basically the same as shown in Figure 4 except that for ISI-87 slightly positive deviations from additivity occur at high PPO contents.

**Systems with Two Hard-Phase Glass Transitions.** Figure 5 shows glass transition behavior for blends of PPO with four copolymers that do not exhibit a single hard-phase  $T_g$  at all compositions. Each system shows a single  $T_g$  up to a critical PPO content, beyond which two hard-phase transitions are evident by DSC. The lower transition results from a PS-rich phase while the higher one indicates a PPO-rich phase. The upper hard-phase transitions are plotted for SEBS-5, SEBS-7, and SEBS-8, while both the upper and lower hard-phase transitions are shown for SEBS-10. Data points are averages from several scans of the same sample. In all cases, the lower glass transition increases with the addition of PPO (as illustrated in Figure 5 for SEBS-10 and shown elsewhere<sup>30</sup> for the other blends), indicating that considerable PPO is solubilized in the PS microphase.

SEBS-5 has the lowest PS molecular weight and PS content of all copolymers studied. From the results in Figure 5b, it is apparently the least capable of solubilizing PPO in the PS microphase. The upper  $T_g$  is detectable at low PPO concentrations and remains very near that for pure PPO as the fraction of PPO in the blend decreases. It follows that this transition reflects an essentially pure PPO phase, perhaps with PS chains lining the boundaries but not affecting the  $T_g$  significantly. No trend with PPO molecular weight is apparent for either the upper or lower  $T_g$ . Standard deviations of the lower transition (not shown) for blends with this copolymer were larger than for other blends.

Results for blends with SEBS-7 and SEBS-8 are presented in parts c and d of Figure 5, respectively. The PS

Table III  
Maximum PPO Solubilization in PS Microphases<sup>a</sup>

	SEBS-5	SEBS-7	SEBS-8	SEBS-10	SBS-15	SEBS-29C	SEBS-29E	ISI-87
PPO-24	15	60	65	75	100	100	100	100
PPO-31	50	60	65	60	100	100	100	100
PPO-33	40	60	45	75	100	100	100	100
PPO-34	40	60	65	75	100	100	100	100
PPO-39	40	60	65	75	100	100	100	100

<sup>a</sup> The numbers are the average of the highest composition displaying a single hard-phase transition and the lowest composition displaying two hard-phase transitions expressed as weight percent PPO in the blend on a rubber-free basis.

molecular weights of these copolymers are very similar although their  $T_g$  behaviors are rather different. Both show a smaller composition region over which two  $T_g$ s are detected than does SEBS-5. The glass transition of the pure SEBS-8 copolymer was impossible to interpret unambiguously during normal scans. An end point was visible but the onset was masked by the broad melting endotherm of the slightly crystallized rubber phase. A value of 86 °C was observed repeatably after extensive annealing; however, short-term annealing of other copolymers was found to change the value of  $T_g$  by as much as  $\pm 4$  °C. The upper transition for SEBS-7 blends changes very little with PPO content and consequently reflects a nearly pure PPO phase. On the other hand, for SEBS-8 this transition temperature decreases noticeably from the  $T_g$  of pure PPO. Probably some PS segments are mixed into the PPO-rich phase.

Results for the highest molecular weight copolymer of this group, SEBS-10, are shown in Figure 5a. These blends have a single hard-phase transition except for a small composition region at 80% PPO and above where two  $T_g$ s are evident. The lower  $T_g$ s follow the trend expected for miscible PPO-PS blends up to about 70% PPO. The upper  $T_g$ s decrease with decreasing PPO content but are above the Fox prediction. The behavior here appears to be approaching the sigmoidal-type relation noted for SEBS blends with a single hard-phase  $T_g$ .

The composition range over which a single transition is detected is greater the higher the PS block molecular weight. Table III lists PPO compositions for each blend system at which the mixed phase becomes saturated with PPO homopolymer. These values were estimated by an average of the highest composition displaying a single hard-phase transition and the lowest composition displaying two hard-phase transitions. For low PS block molecular weights the single hard-phase region is small. For higher PS block molecular weights, it increases to the limit where only one transition is detected for all concentrations as shown in Figure 2. The extent of the composition region for which a single  $T_g$  is observed seems to be rather independent of PPO molecular weight. On the basis of previous reports,<sup>1-4</sup> one might expect more PPO to be solubilized into the PS microphase of a block copolymer the lower the PPO molecular weight; however, this was not observed. There is some evidence to suggest that to a slight extent, the opposite may be true. Polydispersity of the PPO may affect the transition behavior with some fractionation of the PPO occurring, but no clear evidence of this effect can be confirmed by these data.

When the phase containing the PS segments becomes saturated with PPO and an additional PPO-rich hard phase appears, one might expect the composition and  $T_g$  of the saturated phase to remain relatively constant as further PPO is added to the blend. The results in Figure 5a do not strictly adhere to this expectation. However, at PPO contents just below the appearance of the second hard phase, these transitions become very broad as described next. The associated difficulties of defining the

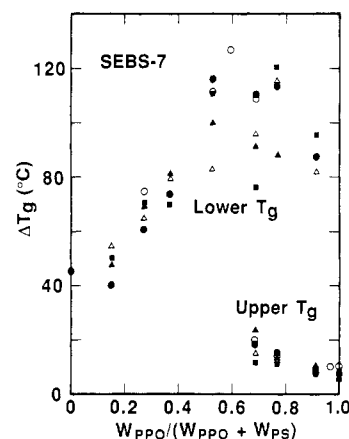


Figure 6. Breadth of the glass transition for the PS-rich phase and the PPO-rich phase versus weight fraction PPO for blends of PPO-24 (●), PPO-31 (▲), PPO-33 (■), PPO-34 (○), and PPO-39 (Δ) with SEBS-7.

temperature location of such broad transitions may account for these observations.

The  $\Delta T_g$ s of the PS phase for the pure copolymers in Figure 5 range from 30 to 50 °C which is much larger than those for the copolymers in Figure 2. The molecular weights of the PS blocks for the copolymers are smaller and, thus, have a larger mixed interphase and possibly a greater degree of mixing of rubbery segments into the PS phases. Transition breadths for the SEBS-7 blend systems are shown in Figure 6. As PPO is added to these copolymers, the hard-phase  $\Delta T_g$  increases sharply until a second hard phase rich in PPO appears. Further additions of PPO cause the breadth of the PS-rich phase to decrease from the maximum value. The location and magnitude of the maximum  $\Delta T_g$  for the PS-rich phase are similar for SEBS-7, SEBS-8, and SEBS-10 blend systems. Breadths for SEBS-5 blends are generally smaller than for blends of the other three copolymers. Formation of two hard phases occurs at a very low PPO content for this copolymer and before the breadth of the transition can become extremely large. The  $\Delta T_g$  for the PS-rich phase is very large for some PPOs and smaller for others, showing no consistent trend with PPO molecular weight. The PS-rich phase at high PPO contents is a very small fraction of the total blend and is probably nonuniform in composition.

Transition breadths for the PPO-rich phase are quite narrow compared to those for the PS-rich phase and increase from the pure PPO value as the fraction of this component decreases.

Figure 7 shows the change in heat capacity at each hard-phase transition noted for blends of PPO with SEBS-5 and SEBS-10 (similar results found for SEBS-7 and SEBS-8 are not shown). These values are expressed in terms of the total hard-phase (PS + PPO) mass. Ideally, these  $\Delta C_p$ s should be proportional to the amount of the phase giving rise to these transitions; however, the difficulty in determining this quantity owing to the dilution of their magnitude by the rubber present and the breadth

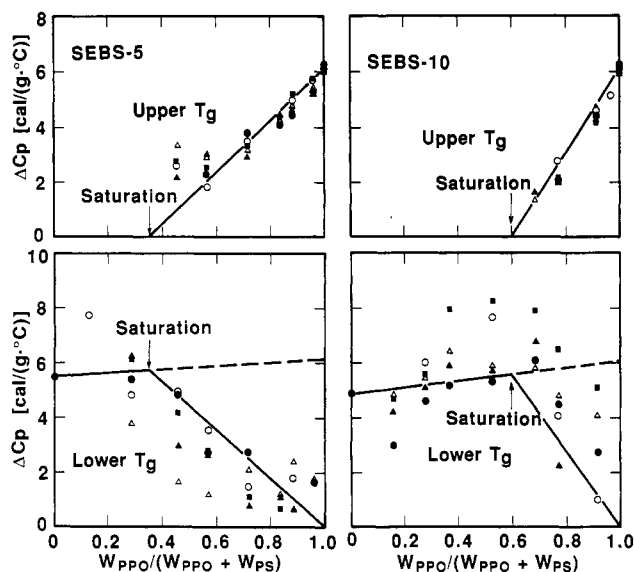


**Figure 7.** Heat capacity change through the PPO-rich  $T_g$  (upper panel) and PS-rich  $T_g$  (lower panel) versus rubber-free weight fraction PPO for the blends of PPO-24 (●), PPO-31 (▲), PPO-33 (■), PPO-34 (○), and PPO-39 (△) with SEBS-5 (left) and SEBS-10 (right). Solid and dashed lines are expected trends described in the text.

of these transitions results in a good deal of scatter. The lines drawn in Figure 7 indicate the behavior expected on the basis of the following interpretation. At low PPO contents there is a single transition whose  $\Delta C_p$  should increase from that of the copolymer PS microphase up to that of pure PPO as seen in Figure 4. This is shown by the solid line at low PPO contents (lower parts of Figure 7) which is continued as a dashed line up to pure PPO from the point where the PPO-rich hard phase appears. From this point, the  $\Delta C_p$  for the PPO-rich phase increases linearly up to that for pure PPO and reflects the proportion of this phase. While the intrinsic value of the heat capacity change for the mixed phase should remain constant from this point on, provided its composition remains fixed, the  $\Delta C_p$  reported is based on total hard-phase mass and must decline to zero at 100% PPO reflecting the decreasing fraction that the fixed amount of this mixed phase contributes to the total mass of the two hard phases. In view of the difficulties associated with measuring the  $\Delta C_p$  mentioned above, the pattern of the experimental results is in satisfactory accord with the physical interpretation associated with the lines drawn in Figure 7. Based on this we can state that at 77% PPO, approximately one-half of the PPO in the blend is in the mixed phase and the other half is in an essentially pure PPO phase for SEBS-7, SEBS-8, and SEBS-10. For SEBS-5 at 77% PPO, about 80% of the PPO is in the PPO-rich phase.

Based on the observed responses of  $T_g$ ,  $\Delta T_g$ , and  $\Delta C_p$ , the phase behavior for these blends depends to a great extent on the molecular weight of the PS block of the copolymer and to a minor extent on the type of rubber in the block copolymer, but it is rather independent of the PPO molecular weight for the range investigated. Any effects associated with the polydispersity of the PPO, copolymer rubber content or type, or copolymer architecture were not controlled or varied extensively enough to discern.

**Effects of Annealing.** In an attempt to assess how far these solution-prepared blends are from an equilibrium state, a limited annealing study was made. Other investigations have used long annealing times at temperatures just above the glassy phase  $T_g$  to approach the equilibrium morphological state for pure copolymers.<sup>31</sup> The free energy

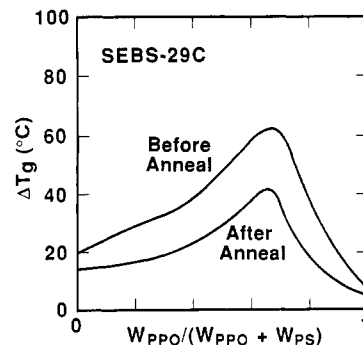


**Figure 8.** Transition breadths before and after annealing for 30 min just below  $T_g$  for blends of PPO with SEBS-29C. Trend is representative for all blends that exhibit a single hard phase.

differences associated with deviations from equilibrium mixing behavior of blends should be much greater than the surface effects for deviations from morphological equilibrium. The latter is beyond the scope of this work. The annealing times in this work were relatively short and of fixed duration as described in the Experimental Section and, therefore, do not constitute an in-depth study. Nevertheless, some general features are mentioned in the following which provide a better understanding of the state of these blends.

The location of the transition midpoints,  $T_g$ , for the blends of Figure 2 (those exhibiting a single hard-phase  $T_g$ ) do not change upon annealing; however, the transitions become significantly less broad after annealing for the blends and the pure components as shown in Figure 8. Only slight changes in  $\Delta C_p$  occur on annealing the blends. The  $\Delta C_p$  for the PS phase of the pure copolymer decreases on annealing. This suggests that some material that contributes to  $\Delta C_p$  before annealing no longer does so after annealing. Some rubber segments present in the interphase and within the PS domains may redistribute into the rubber matrix as a result of annealing. Since blends do not respond similarly, it might be argued that the presence of PPO more fully excludes rubber segments in the as-prepared samples.

The glass transitions for the blends in Figure 5 do show some slight changes on annealing and the general trends are described here. For the PS-rich phase, the variability among the various PPO samples tends to decrease for most compositions. After annealing, transitions indicative of a PPO-rich phase appeared for some compositions where such transitions were not evident before annealing. This may be the result of improved resolution by the DSC after annealing or an actual higher degree of mixing than equilibrium trapped in place by the rapid precipitation from a homogeneous solution. The transition breadths for the PS-rich phase do not change noticeably for compositions that exhibit two hard phases prior to annealing. However, for compositions that show only one hard phase (and especially those that develop a PPO-rich phase on annealing) the breadth of the mixed phase transition decreases on annealing. As pointed out previously, the  $\Delta T_g$  at the PPO saturation limit may be inflated due to overlap of two transitions. Resolution of two hard phases after annealing having much smaller  $\Delta T_g$ s is consistent with this. For blends, the  $\Delta C_p$  do not change on annealing for the PPO-rich phase, but small changes are seen for the PS-rich phase. However, the general trends are similar after annealing to those before.

On annealing, mixed PPO-PS phases generally become more homogeneous, based on the sharpening of the  $T_g$ , and resolution of two hard phases at the saturation limit is more clear for several systems. However, that the blends



do not change greatly on annealing indicates that this preparation method gives nearly equilibrium phase behavior for these systems.

### Summary

Table III summarizes the essence of this investigation by giving an estimate of the maximum amount of PPO that can be incorporated in the PS microphases of a series of triblock copolymers without forming a separate PPO-rich phase detectable by DSC. These results, estimated from the glass transition behavior shown in Figures 2 and 5, are averages to the nearest 5% of the lowest composition exhibiting a PPO-rich transition and the highest composition exhibiting only a PS-rich transition. As expected, the amount of PPO that can be solubilized is a strong function of the molecular weight of the PS segments of the block copolymer; however, it does not seem to be significantly affected by the molecular weight of the PPO over the range examined. The latter finding is in sharp contrast to what has been well-established in the literature when the homopolymer is polystyrene.<sup>1-4</sup> Furthermore, at the homopolymer molecular weights shown in Table III, considerably less polystyrene would have been solubilized in the PS microphases of these copolymers than was observed for PPO. We believe these differences stem from the exothermic mixing of PPO and PS units which amounts to an additional driving force for solubilization relative to the case where the homopolymer is polystyrene. In the companion paper,<sup>32</sup> a simple model confirms the importance of the PPO-PS heat of mixing relative to other thermodynamic contributions to this process. The trends predicted by this model agree rather well with the experimental results described here and summarized by Table III.

The results described here and by others<sup>10,11</sup> point to opportunities for raising the softening temperature or otherwise modifying the properties of the microphases of block copolymers through blending with homopolymers that have favorable interactions with these segments. This might be useful as a means for increasing the upper use temperature of some thermoplastic elastomers where the hard phase is dispersed in a rubber matrix. These issues also relate to rubber toughening at the other composition extreme, where the hard phase is the matrix.

In an earlier paper<sup>15</sup> we reported briefly on the phase morphology of one of the blend systems described here and showed evidence by electron microscopy for the presence of a small amount of a PPO phase that was not detected thermally or mechanically. More work is needed in these areas to map more fully the morphological and detailed phase behaviors that are possible with such systems. In addition, it would be instructive to examine the state of mixing within the microphases and the interphase by using other techniques. More detailed investigations of any role of rubber block size, type, or location on the solubilization process are also in order. Finally, it would be interesting to vary the strength of the homopolymer-block segment

interaction parameter to better assess the role of this additional driving force for solubilization.

**Acknowledgment.** We express appreciation to Shell Development Co. and to General Electric Co. for generously providing materials, to Phillips Petroleum Foundation for a fellowship, and to General Motors Research Laboratories for partial financial support.

**Registry No.** PPO (SRU), 24938-67-8; PPO (homopolymer), 25134-01-4; (S)(butadiene)(isoprene) (block copolymer), 105729-79-1.

### References and Notes

- (1) Riess, V. G.; Kohler, J.; Tournut, C.; Bandaret, A. *Makromol. Chem.* **1967**, *101*, 58.
- (2) Inoue, T.; Soen, T.; Hashimoto, T.; Kawai, H. *Macromolecules* **1970**, *3*, 87.
- (3) Ptaszynski, B.; Terrisse, J.; Skoulios, A. *Makromol. Chem.* **1975**, *176*, 3483.
- (4) Toy, L.; Miinomi, M.; Shen, M. J. *Macromol. Sci.-Phys.* **1975**, *B11*(3), 281.
- (5) Meier, D. J. *Polym. Prepr. (Am. Chem. Soc., Div. Polym. Chem.)* **1977**, *18*(1), 340.
- (6) Rigby, D.; Lim, J. L.; Roe, R.-J. *Macromolecules* **1985**, *18*, 2269.
- (7) Whitmore, M. D.; Noolandi, J. *Macromolecules* **1985**, *18*, 2486.
- (8) de la Cruz, M. O.; Sanchez, I. C. *Macromolecules* **1987**, *20*, 440.
- (9) Xie, H.; Liu, Y.; Jiang, M.; Yu, T. *Polymer* **1986**, *27*, 1928.
- (10) Kambour, R. P. (to General Electric Co.) U.S. Patent 3639 508, Feb 1, 1972.
- (11) Shultz, A. R.; Beach, B. M. *J. Appl. Polym. Sci.* **1977**, *21*, 2305.
- (12) Meyer, G. C.; Tritscher, G. E. *J. Appl. Polym. Sci.* **1978**, *22*, 719.
- (13) Hansen, D. R. (to Shell Development Co.) U. S. Patent 4141 876, Feb 26, 1979.
- (14) Tucker, P. S.; Barlow, J. W.; Paul, D. R. *J. Appl. Polym. Sci.* **1987**, *34*, 1817.
- (15) Tucker, P. S.; Barlow, J. W.; Paul, D. R. *Macromolecules* **1988**, *21*, 1678.
- (16) Shultz, A. R.; Gendron, B. M. *J. Appl. Polym. Sci.* **1972**, *16*, 461.
- (17) Bair, H. E. *Polym. Eng. Sci.* **1970**, *10*, 247.
- (18) MacKnight, W. J.; Stoelting, J.; Karasz, F. E. *Adv. Chem. Ser.* **1971**, *99*, 29.
- (19) Paul, D. R.; Barlow, J. W. *J. Macromol. Sci.* **1980**, *C18*(1), 109.
- (20) Holden, G.; Bishop, E. T.; Legge, N. R. *J. Polym. Sci., Part C* **1969**, *26*, 37.
- (21) Olabisi, O.; Robeson, L. M.; Shaw, M. T. *Polymer-Polymer Miscibility*; Academic: New York, 1979; Chapter 3.
- (22) Fetters, L. J.; Meyer, B. H.; McIntyre, D. J. *J. Appl. Polym. Sci.* **1972**, *16*, 2079.
- (23) Hsiue, G.-H.; Ma, M.-Y. M. *Polymer* **1984**, *25*, 882.
- (24) Granger, A. T.; Wang, B.; Krause, S.; Fetters, L. J. *Adv. Chem. Ser.* **1986**, *211*, 127.
- (25) Guar, U.; Wunderlich, B. *Macromolecules* **1980**, *13*, 1618.
- (26) Granger, A. T.; Krause, S. *Macromolecules* **1987**, *20*, 1421.
- (27) Fox, T. G. *Bull. Am. Phys. Soc.* **1956**, *2*, 123.
- (28) Fried, J. R.; Lorenz, T.; Ramdas, A. *Polym. Eng. Sci.* **1985**, *25*, 1048.
- (29) MacKnight, W. J.; Karasz, F. E.; Fried, J. R. In *Polymer Blends*; Paul, D. R., Newman, S., Eds.; Academic: New York, 1978; Vol. I, p 226.
- (30) Tucker, P. S. Doctoral Dissertation, University of Texas, 1988.
- (31) Thomas, E. L.; Alward, D. B.; Kinnig, D. J.; Martin, D. C.; Handlin, D. L.; Fetters, L. J. *Macromolecules* **1986**, *19*, 2197.
- (32) Tucker, P. S.; Paul, D. R. *Macromolecules*, following paper in this issue.